Correspondence between some wave patterns and Lissajous figures

2006 J. Phys. A: Math. Gen. 39 13285

(http://iopscience.iop.org/0305-4470/39/42/006)

INSTITUTE OF PHYSICS PUBLISHING JOURNAL OF PHYSICS A: MATHEMATICAL AND GENERAL

J. Phys. A: Math. Gen. **39** (2006) 13285–13293 doi:10.1088/0305-4470/39/42/006

Correspondence between some wave patterns and Lissajous figures

K J Górska, A J Makowski and S T Dembiński

Institute of Physics, Nicolaus Copernicus University, ul. Grudziądzka 5, 87-100 Toruń, Poland

E-mail: amak@fizyka.umk.pl

Received 11 July 2006, in final form 30 August 2006
Published 4 October 2006
Online at stacks.iop.org/JPhysA/39/13285

Abstract

We study the connections between some specially entangled *stationary* states and the classical periodic trajectories of two non-interacting oscillators. The latter are well-known Lissajous figures, which are shown to run precisely over the apogees of their corresponding probability distributions in the above states. We propose in this work a very simple criterion enabling us to obtain the best agreement between the quantum and the classical images. Finally, our results are successfully applied to the interpretation of some experimentally observed wave patterns.

PACS numbers: 03.65.Vf, 03.65.Ge, 03.65.Fd

(Some figures in this article are in colour only in the electronic version)

1. Introduction

Study of the mutual relationships between quantum and classical descriptions of various physical systems has a long and fascinating history, which began with the onset of quantum mechanics. For many years the studies were mostly theoretical ones. However, with the recent achievements in the field of developing sophisticated experimental techniques, the verification and successful confrontation of the theoretical suppositions with the experimental results has been enabled.

The problems examined in this way include among others real-time measurements of the single atom trajectories [1], Wigner function tests [2, 3], research on when classical and quantum evolutions agree, that is Ehrenfest's time measurements [4], or the examination of quantum–classical transitions in nonlinear dynamical systems [5]. Moreover, one of the most intensively studied phenomena is the quantum systems' decoherence [6].

Contemporary pico- and femtosecond laser techniques also allow for the atoms to be prepared in such a way that the well-localized wave packets move along classical orbits in

highly excited Rydberg states [7, 8]. There are also interesting theoretical considerations of such states in the hydrogen atom [9] and in rotating molecules [10].

In other types of experiments an ideal localization of quantum states is obtained even for low values of quantum numbers. Specifically, this concerns a series of the very recent papers [11–14], where using a fiber-coupled diode-end-pumped microchip laser, certain pictures (wave patterns) are obtained which are perfectly localized on classical trajectories of various, even very complex, shapes. The images consist of a number of bright and dark spots falling onto the well-known classical Lissajous figures, also rarely referred to as the Bowditch curves.

As shown in [15] by choosing the quantum states as the $SU(2)$ like coherent states in the Schwinger representation, we are able to reproduce the experimentally observed patterns. The unsolved problem, however, is that the formulae [11, 12, 15] proposed for this purpose so far were only found due to numerical adjustments. Moreover, we have proved recently [16] that the formulae need some corrections in order to have the classical Lissajous figures running exactly over apogees of the experimental patterns. This is especially important for low values of quantum numbers. That is why, we attempt to give in this work a possibly very simple solution to the above problems.

Most of the paper is devoted to the study of close relationships of some probability densities to the classical Lissajous figures in connection with the recently published wave patterns. Our main goal is to find the best combination of the 2D harmonic oscillator eigenstates to get the correspondence between the quantum state and several classical figures as close as possible.

This paper is organized as follows: in section 2 we present the exact form of the chosen entangled state for the system of two non-interacting harmonic oscillators; in section 3 we derive suitable quantum–classical connections, i.e., the dependence of the amplitude and phase of the classical motion on the entangled state; in section 4 we compare our theory with the mentioned experimental patterns and sum up our conclusions.

2. Construction of the state

Based on the well-known and often utilized fact that the paraxial wave equation for the spherical laser resonators is formally identical with the two-dimensional (2D) Schrödinger equation for the harmonic oscillator [17–19], we start with the Hamiltonian $H(x, y) = H(x)+H(y)$, where $H(x) = p_x^2/(2m_x) + (1/2)m_x\omega_x^2x^2$ and similarly for $H(y)$. Its normalized eigenfunctions have the well-known form

$$\Phi_{m,n}(x, y) = N_{m,n}H_m(x\sqrt{2}/X)H_n(y\sqrt{2}/Y)\exp[-(x/X)^2 - (y/Y)^2], \quad (1)$$

where $X = \sqrt{2\hbar/(m_x\omega_x)}$, $Y = \sqrt{2\hbar/(m_y\omega_y)}$, $N_{m,n} = (XY\pi m!n!2^{m+n-1})^{-1/2}$, and the eigenvalues associated with the state read $E_{m,n} = \hbar\omega_x(m + 1/2) + \hbar\omega_y(n + 1/2)$. If we introduce some integers p and q such that $\omega_x : \omega_y = q : p$, then

$$E_{m,n} = \hbar\omega[q(m + 1/2) + p(n + 1/2)], \quad (2)$$

with ω being a common factor of both frequencies.

Generalizing the spin-type coherent states [20, 21], we take the following finite combination of the oscillator states:

$$\Psi_N^{p,q}(x, y, \tau) = \frac{1}{(1 + |\tau|^2)^{N/2}}\sum_{k=0}^{N}\binom{N}{k}^{1/2}\tau^k\Phi_{pk,q(N-k)}(x, y), \quad (3)$$

where τ is, in general, a complex parameter taken in the polar form as $\tau = A\exp(\mathrm{i}\phi)$.

For further reference, we can calculate the expectation values of several operators in the above state [15]:

$$\langle x^2\rangle = \left(\frac{A^2}{1+A^2}pN+\frac{1}{2}\right)\frac{X^2}{2}, \qquad \langle y^2\rangle = \left(\frac{1}{1+A^2}qN+\frac{1}{2}\right)\frac{Y^2}{2}, \tag{4}$$

and

$$E_x = \langle H(x)\rangle = q\left(\frac{pN|\tau|^2}{1+|\tau|^2}+\frac{1}{2}\right)\hbar\omega, \tag{5}$$

$$E_y = \langle H(y)\rangle = p\left(\frac{qN}{1+|\tau|^2}+\frac{1}{2}\right)\hbar\omega. \tag{6}$$

Formally, the state (3) is a superposition of the eigenstates $\Phi_{pk,q(N-k)}(x, y)$ which are $(N+1)$-fold degenerate for an integer $N > 0$, and their eigenvalues are $E_N = \hbar\omega[pqN+(p+q)/2] = E_x + E_y$.

As shown previously [11–16], the state (3) for the $q : p$ anisotropic oscillators may be considered as the proper choice for reproducing the sharp transverse patterns well localized on the Lissajous figures observed in a cavity of a suitable length. Earlier the representation was successfully used [22, 23] for the construction of the wavefunctions associated with the classical elliptical orbits in a 2D isotropic harmonic oscillator.

Our goal, however, is to find close connections between the patterns and the corresponding classical Lissajous figures, represented by the set of equations

$$x = A_x\cos(\omega_x t+\alpha_x), \qquad y = A_y\cos(\omega_y t+\alpha_y). \tag{7}$$

By the close connection, we mean the relations, as exact as possible, between the amplitudes A_x, A_y and the phase shifts α_x, α_y of a classical orbit, on the one hand, and the free parameters of the quantum state (3), i.e., the amplitude A and the phase ϕ of its complex quantity τ, on the other hand. The quantum–classical connection would be perfect, if classical figures obtained in this way were running over apogees of the probability density $\left|\Psi_N^{p,q}(x, y, \tau)\right|^2$ for every N. Obviously, the number of bright and dark spots, as well as the shapes and sizes of the formally created patterns and those of the mentioned experiments, should be the same.

3. Quantum–classical connection

For making a connection of the quantum state (3) with the classical periodic Lissajous figures we restrict ourselves to the relatively prime values of p and q only. Then, the images of $|\Psi_N^{p,q}(x, y, \tau)|^2$ are localized on a single, non-repeated orbit [15].

3.1. Amplitudes

The previously proposed [11, 12, 15] connections of the classical amplitudes A_x and A_y in (7) with the state of equation (3) were adjusted to the relations

$$A_x = \sqrt{2\langle x^2\rangle}, \qquad A_y = \sqrt{2\langle y^2\rangle}. \tag{8}$$

We can derive them demanding that

$$\langle H(i)\rangle = E_c(i), \qquad i = x, y, \tag{9}$$

where $E_c(i)$ is the total energy of the ith classical oscillator, and for the quantum energies, we have $\langle H(x)\rangle = m_x\omega_x^2\langle x^2\rangle$ and $\langle H(y)\rangle = m_y\omega_y^2\langle y^2\rangle$. Assumption (9) works very well for

high quantum numbers N, and as has been proved in [16], for low values it should be modified to yield

$$\langle H(i)\rangle = E_c(i) + (1/2)\hbar\omega_i, \qquad i = x, y. \tag{10}$$

As a result, the corrected amplitudes follow as

$$A_x = \sqrt{2\langle x^2\rangle - \hbar/(m_x\omega_x)}, \qquad A_y = \sqrt{2\langle y^2\rangle - \hbar/(m_y\omega_y)}. \tag{11}$$

3.2. Phase shifts

The task now is to find relations between the continuous parameter τ, i.e., the values of A and ϕ in the state $\Psi_N^{p,q}(x, y, \tau)$ of equation (3), and the phase shifts α_x and α_y of the classical orbits in (7).

The dependence on A can be made trivial if we assume in (5) and (6) that $E_x = E_y$. Then, we have

$$A^2 = |\tau|^2 = \frac{pqN + \frac{1}{2}(p-q)}{pqN - \frac{1}{2}(p-q)}, \tag{12}$$

which for a large enough N is close to unity. Thus, the choice of $A = 1$ guarantees roughly the same energies of both oscillators, and seems to be well suited to the study of the quantum–classical connections.

The problem of the parameter ϕ and its relation to the phase shifts α_x and α_y is much more subtle. Let us note first that the Lissajous figures of equation (7) are invariant with respect to changes in the phases α_x and α_y provided the quantity $\varphi = q\alpha_y - p\alpha_x$ is conserved modulo 2π. In particular, a pair of (α_x, α_y) may be replaced by p pairs $(p > q)$ of $(\tilde{\alpha_x}, \tilde{\alpha_y})$ such that $\tilde{\alpha_x} = -(\varphi - 2\pi qn)/p$ with $n = 0, 1, 2, \ldots, p-1$, and $\tilde{\alpha_y} = 0$. We shall call the pairs with $\tilde{\alpha_y} = 0$ 'the prime representation' of phases.

Now, we adopt the following procedure. Knowing τ, i.e. ϕ, since we have assumed $|\tau|^2 = A^2 = 1$, we look for phase shifts α_x and α_y which maximize the integral $I[x, y] = (1/l)\oint f(x, y)\,\mathrm{d}s$ with $l = \oint \mathrm{d}s$, where x and y belong to the chosen Lissajous figure, $f(x, y) = \left|\Psi_N^{p,q}(x, y, \tau)\right|^2$, and the closed path integrals are taken along the figure. When the classical orbits are given in the parametric form, like in (7), then

$$I[x(t), y(t)] = \frac{1}{l}\int_0^T f[x(t), y(t)]\sqrt{\dot{x}^2 + \dot{y}^2}\,\mathrm{d}t, \qquad l = \int_0^T \sqrt{\dot{x}^2 + \dot{y}^2}\,\mathrm{d}t, \tag{13}$$

and the symbol T stands for the period of used functions. For $\alpha_x^{\max}$ and $\alpha_y^{\max}$, which maximize I, the Lissajous figures run over the apogees of the corresponding probability distributions. Note that there are many such pairs of $\alpha^{\max}$'s but they can be reduced to one of the p pairs in the 'prime representation' $\tilde{\alpha}_x^{\max} = -(\varphi^{\max} - 2\pi qn)/p$ and $\tilde{\alpha}_y^{\max} = 0$ with $\varphi^{\max} = q\alpha_y^{\max} - p\alpha_x^{\max}$. In general, the above procedure can only be performed numerically.

Trying to get a more analytical approach for the determination of α's, we noticed that there exists a quantity which is associated with a Lissajous figure and depends on α's only via the invariant φ mentioned above. This quantity, which we denote as $\overline{x^p y^q}$, equals

$$\overline{x^p y^q} = \frac{1}{T}A_x^p A_y^q \int_0^T \cos^p(q\omega t + \alpha_x)\cos^q(p\omega t + \alpha_y)\,\mathrm{d}t. \tag{14}$$

The integral in (14) can be performed exactly, and we have

$$\overline{x^p y^q} = 2^{-p-q+1}A_x^p A_y^q \cos(\varphi). \tag{15}$$

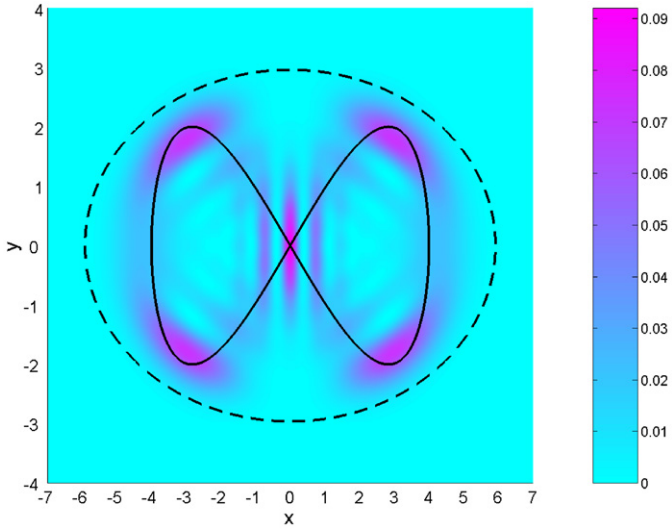

Figure 1. A density plot of $|\Psi_N^{p,q}(x, y, \tau)|^2$ for $p = 2, q = 1, N = 8, \phi = \pi/2, X = \sqrt{2/q}$, $Y = \sqrt{2/p}, \hbar/(m_x\omega) = \hbar/(m_y\omega) = 1, A = 1$ and $\omega = 1$. The corresponding classical figure (full line) is plotted from equations (7), (11), (4) and (21). The dashed line is an ellipse and represents the classically allowed area. Dimensionless units are used.

Looking at this classical average, one is tempted to calculate the corresponding quantum average $\langle x^p y^q \rangle$. The calculations become easily tractable if the bosonic creation and annihilation operators are used: $a^{\pm} = \sqrt{m_x\omega_x/(2\hbar)}x \mp \sqrt{\hbar/(2m_x\omega_x)}(\mathrm{d}/\mathrm{d}x)$, $[a^-, a^+] = 1, b^{\pm} = \sqrt{m_y\omega_y/(2\hbar)}y \mp \sqrt{\hbar/(2m_y\omega_y)}(\mathrm{d}/\mathrm{d}y)$, $[b^-, b^+] = 1$ and $[a^{\pm}, b^{\pm}] = [a^{\mp}, b^{\pm}] = 0$. From these relations, we get $x = \sqrt{\hbar/(2m_x\omega_x)}(a^- + a^+)$ and $y = \sqrt{\hbar/(2m_y\omega_y)}(b^- + b^+)$. Now, observe that the only nonzero contributions to the average $\langle x^p y^q \rangle$ come from the terms proportional to $(a^-)^p(b^+)^q$ and $(a^+)^p(b^-)^q$. Then, after some algebra, we obtain

$$\langle x^p y^q \rangle = 2^{-p-q+1} X^p Y^q (1 + |\tau|^2)^{-N} S_N^{(p,q)}(A) \cos(\phi), \tag{16}$$

where

$$S_N^{(p,q)}(A) = \sum_{k=0}^{N} \binom{N}{k}^{1/2} \binom{N}{k+1}^{1/2} A^{2k+1} \sqrt{(pk+1)(pk+2)\cdots(pk+p)} \times \sqrt{[q(N-k)][q(N-k)-1]\cdots[q(N-k)-q+1]}. \tag{17}$$

Examining relations between both averages we observe the following.

(i) There are such sets of the parameters N, p, q and τ that for a given value of ϕ the value of φ, which is necessary for the equality $\langle x^p y^q \rangle = \overline{x^p y^q}$ to hold, does not exist.

(ii) If this is not the case, then the relation between ϕ and φ stems from the assumed equality $\langle x^p y^q \rangle = \overline{x^p y^q}$, i.e., we know the value of φ. Let it be $\varphi = \varphi^{\mathrm{eq}}$. A Lissajous figure is given now by the prime set of $\tilde{\alpha}$'s represented by $\tilde{\alpha}_x^{\mathrm{eq}} = -(\varphi^{\mathrm{eq}} - 2\pi qn)/p, \tilde{\alpha}_y^{\mathrm{eq}} = 0$. Values of the integrals I obtained for $\varphi = \varphi^{\max}$ and $\varphi = \varphi^{\mathrm{eq}}$ differ and $I(\varphi^{\max}) > I(\varphi^{\mathrm{eq}})$ in general. The Lissajous figure generated by φ^{eq} does not as nicely follow the 'ridge path' of the quantum probability as that generated by $\varphi^{\max}$. An example of this kind is presented in figure 1. Additionally, we have plotted in this figure the classically allowed

region (the dashed line) of the (x, y) space corresponding to the energy E_N defined in section 2. Obviously, it is an ellipse $x^2/a^2 + y^2/b^2 = 1$ with $a^2 \equiv 2E_N/\left(m_x\omega_x^2\right)$ and $b^2 \equiv 2E_N/\left(m_y\omega_y^2\right)$. In the dimensionless system of units used in our plots, its major and minor semi-axes are $a = 5.92$ and $b = 2.96$, respectively.

(iii) There are cases when our knowledge of both averages is satisfactory to prove that $\phi = \varphi$. We meet such situation when

(1) $\langle x^p y^q\rangle = \overline{x^p y^q} = 0$, and then it follows that $\phi = \varphi = q\alpha_y - p\alpha_x = (2k+1)(\pi/2)$, $k = 0, 1, 2, \ldots$;

(2) the factors of $\cos(\varphi)$ in (15), and of $\cos(\phi)$ in (16), are equal. It can be proved that such situation occurs when $p = q = 1$ and then $\phi = \varphi = \alpha_x - \alpha_y$. In this case, the sum in (17) is simply $S_N^{(1,1)}(A) = NA(1+A^2)^{N-1}$, and then, with the help of (16), (15), (11) and (4), we can prove that both averages are equal to each other, provided $\phi = \alpha_x - \alpha_y$, and we have for them $ANXY/[2(1+A^2)]$. Unfortunately, we were not able to perform formally the sum over k in (17) for arbitrary coprime values of p and q.

The question which arises now is whether Lissajous figures with $\tilde{\alpha_x} = -(\phi - 2\pi qn)/p, \tilde{\alpha}_y = 0$ are the same as those with $\tilde{\alpha}_x^{\max}$ and $\tilde{\alpha}_y = 0$. The positive answer, supported by an exact analytical calculation, can be given when both conditions 1 and 2 are simultaneously fulfilled. Then, $\alpha_x - \alpha_y = \pm\pi/2 = \phi$ and $\left|\Psi_N^{1,1}(x, y, \tau = \pm\mathrm{i})\right|^2$ may be written in a closed form [16]

$$\left|\Psi_N^{1,1}(x, y, \tau = \pm\mathrm{i})\right|^2 = \left(\frac{m\omega}{\hbar}\right)^{N+1} \frac{(x^2+y^2)^N}{\pi N!} \exp\left[-\frac{m\omega}{\hbar}(x^2+y^2)\right]. \tag{18}$$

The trajectory running over the maximum of the probability density is given by $x = \sqrt{N\hbar/(m\omega)}\sin(\omega t)$, $y = \sqrt{N\hbar/(m\omega)}\cos(\omega t)$. The same trajectory can be derived from the integrals (13). To this end, let us take $x = \sqrt{N\hbar/(m\omega)}\cos(\omega t + \alpha_x)$ and $y = \sqrt{N\hbar/(m\omega)}\cos(\omega t + \alpha_y)$, and use two identities $\cos^2(\alpha)+\cos^2(\beta) = 1+\cos(\alpha+\beta)\cos(\alpha-\beta)$ and $\sin^2(\alpha)+\sin^2(\beta) = 1-\cos(\alpha+\beta)\cos(\alpha-\beta)$. Then, the first of integrals (13) takes the form

$$\begin{aligned} J \equiv Il = \left(\frac{m\omega}{\hbar}\right)^{1/2} \frac{N^N}{\pi N!} \int_0^{2\pi} &[1+\cos(2\omega t+\alpha_x+\alpha_y)\cos(\alpha_x-\alpha_y)]^N \\ &\times \sqrt{N[1-\cos(2\omega t+\alpha_x+\alpha_y)\cos(\alpha_x-\alpha_y)]} \\ &\times \exp\{-N[1+\cos(2\omega t+\alpha_x+\alpha_y)\cos(\alpha_x-\alpha_y)]\}\,\mathrm{d}t. \end{aligned} \tag{19}$$

Obviously, its maximum value is given for $\alpha_x - \alpha_y = \pm\pi/2$.

That is why, we have $J_{\max} = 2[(m\omega)/\hbar]^{1/2} N^{N+1/2}\exp(-N)/N!$, which, after dividing by the length of the circle $x^2+y^2 = N\hbar/(m\omega)$, i.e., by $l = \int_0^{2\pi}\sqrt{\dot{x}^2+\dot{y}^2}\,\mathrm{d}t = 2\pi[N\hbar/(m\omega)]^{1/2}$, leads to

$$I_{\max} = \left(\frac{m\omega}{\hbar}\right)\frac{N^N\,\mathrm{e}^{-N}}{\pi N!}. \tag{20}$$

With the phase shifts found above, the Lissajous figure (the circle) lies exactly on the maximum of the probability density (18) and the value of the distribution at the maximum is given in (20).

For p and q different from unity, finding the values of α_x and α_y, which maximize the integral for I in (13) for fixed values of the amplitudes A_x and A_y, can only be done numerically. We have checked in this way that for $\phi = \pi/2$ or $\phi = 0$, and arbitrary values of p and q, the approximate relation $I(\varphi^{\max}) \cong I(\varphi = \phi)$ holds and the approximation works very well. In other words, maximizing the Lissajous figures in the prime basis is characterized by

$$\tilde{\alpha}_x = -\phi/p, \qquad \tilde{\alpha}_y = 0, \tag{21}$$

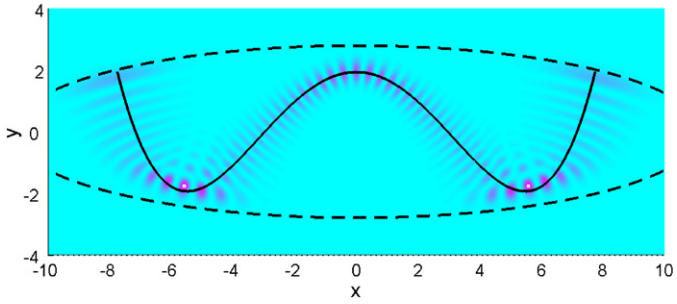

Figure 2. As in figure 1 but for $p = 4, q = 1, N = 15$ and $\phi = 0$.

which were previously guessed [15] from numerical adjustments only. Note that different numbers of the prime representation, i.e. $\tilde{\alpha}_x$, for consecutive n, differ themselves by $2\pi qn/p$ and therefore equations (21) are valid for all n (ϕ is taken modulo π). For values of ϕ different from 0 or $\pi/2$, maximizing values of $\tilde{\alpha}$'s do not agree that well with equations (21).

If p and q are not coprime and have a common factor M, as for example for $p : q = 3 : 3$, then, as observed in [15], the plots of $\left|\Psi_N^{p,q}(x, y, \tau)\right|^2$ do not correspond to a single orbit but to an ensemble of classical periodic orbits. With M assumed as the number of such orbits, they can be obtained from the equations

$$\begin{aligned} x_k(t) &= \sqrt{2\langle x^2\rangle - \hbar/(m_x\omega_x)}\cos(q\omega t - \phi_k/p), \\ y_k(t) &= \sqrt{2\langle y^2\rangle - \hbar/(m_y\omega_y)}\cos(p\omega t), \end{aligned} \tag{22}$$

where $\phi_k = \phi + 2\pi k$ with $k = 0, 1, 2, \ldots, M-1$. They constitute an improved version of equations (9) of [15], where an illustration for the point is also given. We should point out that the correction terms $\hbar/(m_i\omega_i)$, $i = x, y$, are important only for low values of N.

4. Comparison with experiment and conclusions

Our formulae can now be used for (i) the reconstruction of the experimentally obtained patterns, and (ii) for the study of the quantum–classical correspondence. We have chosen for this purpose the first two photos in figure 2 of [11] or (*a*) and (*b*) in figure 2 of [12]. The two images can be reconstructed from $\left|\Psi_N^{p,q}(x, y, \tau = A\exp(\mathrm{i}\phi))\right|^2$ for $p = 4, q = 1, A = 1, \phi = 0$, and for $p = 5, q = 2, A = 1, \phi = 0$, and are presented in figures 2 and 3, respectively. Their shapes and the number of bright and dark spots are reproduced exactly as in [11, 12] if in both cases $N = 15$. The quantum–classical connection is established excellently with the help of (7), (11) and (21) with $\phi = 0$ and $\tilde{\alpha}_y = 0$. Thanks to that, the classical orbits are observed to run exactly over the apogees of the quantum probability distributions. Again, as for figure 1, we have included (dashed lines) ellipses showing classically allowed areas for the eigenenergy E_N in the states $\Phi_{pk,q(N-k)}$ with $k = 0, 1, \ldots, N$. Now, in figure 2, we have $a = 11.18$ and $b = 2.79$, and in figure 3, the values are $a = 8.76$ and $b = 3.50$. The same accurate copies of the remaining experimental images of [11, 12] can be obtained in the similar way. Also, the corresponding Lissajous figures have the expected properties.

Thus, the numerical reconstruction itself of the transverse patterns, which are observed in cavities of a suitable length, is, as shown above, easily done with the help of the state (3). This is the case not only for the patterns associated with the Lissajous orbits considered here but also for some images obtained in square [24] and triangle [25] billiards.

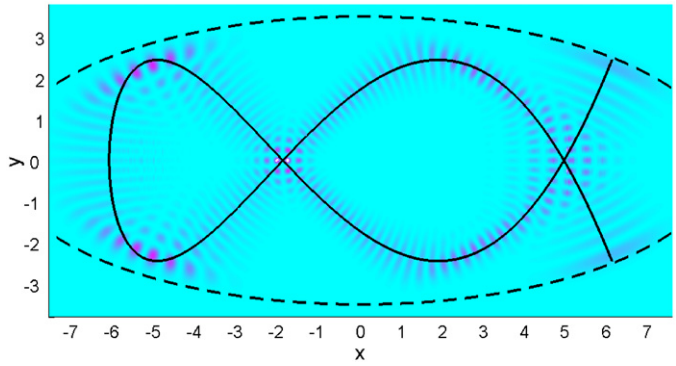

Figure 3. As in figure 1 but for $p = 5, q = 2, N = 15$ and $\phi = 0$.

However, deriving formally exact relations connecting classical trajectories and wave patterns localized on them seems to require more effort, especially for complex periodic orbits like the Lissajous ones. Our approach to this problem is based on two assumptions, formalized by (10) and the ergodic-like assumption, which constitute an alternative to the approach proposed in [15] (cf also [26]). As we have proved in section 3, both assumptions are obeyed exactly for an arbitrary N, in the case of $p = q = 1$. For other values, the quantum–classical connections are not formally exact but work surprisingly well, which is clearly shown in figures 1–3.

Some of the conclusions we have drawn were based on the method of looking for the maximum of the integral I (equation (13)) with respect to the values of α_x and α_y, having fixed the values of τ, i.e., the parameters A and ϕ of the quantum state in (3). The procedure may also be reversed and we can look for $I_{\max}$ with respect to A and ϕ with α_x and α_y fixed. For this purpose we need to know the sets of (p, q) and (α_x, α_y) of a Lissajous figure. To this end, suppose we have experimental images at our disposal, like those in figures 2 and 3, for example.

The coprime values of p and q can be determined from them by counting the number of common points of the corresponding Lissajous figure (full line) and of the rectangular $x = \pm A_x$ and $y = \pm A_y$. This can be done according to the following rules.

(A) *Open Lissajous figures*. ($\phi = 0 \pmod{2\pi}$). For this case $p = 2\Delta + \delta$, where δ is a number of end points of a figure and Δ is for the remaining points which both are common with the lines $y = A_y$ or $y = -A_y$. The same rule holds for the values of q but now we count the points on the lines $x = A_x$ or $x = -A_x$. Referring to our formula $\tilde{\alpha_x} = -(\varphi - 2\pi qn)/p$ with $n = 0, 1, 2, \ldots, p - 1$, note that for $\varphi = 0 \pmod{2\pi}$ among p values of $\tilde{\alpha_x}$'s there are $\Delta + \delta$ of them which give different values of $\cos(\tilde{\alpha_x})$. Examples of this kind are presented in figures 2 and 3.

(B) *Closed Lissajous figures*. Now, we have $p = \Delta$, since there are no end points in this case, and p is again a number of points where the lines $y = A_y$ or $y = -A_y$ are tangential to the Lissajous figure. The values of q are similarly determined by the number of such points on one of the remaining lines of the rectangular. A suitable example is depicted in figure 1.

As concerns the phase shifts α_x and α_y, we can find them in the following way. First, we locate the point $(x = 0, y = 0)$ in the geometric centre of the mentioned rectangular. Coordinates (x, y) of any point belonging to a Lissajous figure may be taken as $x = A_x \cos(\alpha_x)$ and $y = A_y \cos(\alpha_y)$, where the amplitudes A_x and A_y are determined as described in section 3.1. Thus, we have (α_x, α_y) and hence our invariant $\varphi = q\alpha_y - p\alpha_x$.

Consequently, maximizing the integral for I in (13) may now be done with the found sets of (p, q) and (α_x, α_y). As a result, the parameters A and ϕ of the quantum state in (3) can be calculated.

Concluding, results of both the 'direct' and the 'inverse' procedures are obviously consistent. The latter, which starts from an experimental image and ends with the quantum state, seems to be the most desirable method. Moreover, we believe that our results shed some light on using the energy balance (equation (10)) and the ergodic-like assumption in studying the quantum–classical correspondence.

References

[1] Hood C J, Chapman M S, Lynn T W and Kimble H J 1998 *Phys. Rev. Lett.* **80** 4157
[2] Brida G, Genovese M, Gramegna M, Novero C and Predazzi E 2002 *Phys. Lett.* A **299** 121
[3] Banaszek K, Radzewicz C, Wódkiewicz K and Krasiński J S 1999 *Phys. Rev.* A **60** 674
[4] Cametti F and Presilla C 2002 *Phys. Rev. Lett.* **89** 040403
[5] Habib S, Jacobs K, Mabuchi H, Ryne R, Shizume K and Sundaram B 2002 *Phys. Rev. Lett.* **88** 040402
[6] Żurek W H 2003 *Rev. Mod. Phys.* **75** 715
[7] Maddox J 1994 *Nature* **370** 593
Gaeta Z D, Noel M W and Stroud C R Jr 1994 *Phys. Rev. Lett.* **73** 636
[8] Kaliński M, Eberly J H and Białynicki-Birula I 1995 *Phys. Rev.* A **52** 2460
[9] Białynicki-Birula I and Białynicka-Birula Z 1996 *Phys. Rev. Lett.* **77** 4298
[10] West J A, Gaeta Z D and Stroud C R Jr 1998 *Phys. Rev.* A **58** 186
[11] Chen Y F, Lan Y P and Huang K F 2003 *Phys. Rev.* A **68** 043803
[12] Chen Y F, Huang K F and Lan Y P 2003 *Opt. Lett.* **28** 1811
[13] Chen Y F and Lan Y P 2002 *Phys. Rev.* A **66** 053812
[14] Chen Y F and Lan Y P 2003 *Phys. Rev.* A **67** 043814
[15] Chen Y F and Huang K F 2003 *J. Phys. A: Math. Gen.* **36** 7751
[16] Makowski A J 2005 *J. Phys. A: Math. Gen.* **38** 2299
[17] Kogelnik H and Li T 1966 *Appl. Opt.* **5** 1550
[18] Haus H A 1984 *Waves and Fields in Optoelectronics* (Englewood Cliffs, NJ: Prentice-Hall)
[19] Steuernagel O 2005 *Am. J. Phys.* **73** 625
[20] Novaes M and Gazeau J P 2003 *J. Phys. A: Math. Gen.* **36** 199
[21] Klauder J R and Skagerstam Bo-Sture *Coherent States—Applications in Physics and Mathematical Physics* (Singapore: World Scientific)
[22] De Bièvre S 1992 *J. Phys. A: Math. Gen.* **25** 3399
[23] Pollet J, Méplan O and Gignoux C 1995 *J. Phys. A: Math. Gen.* **28** 7287
[24] Chen Y F, Huang K F and Lan Y P 2002 *Phys. Rev.* E **66** 066210
Chen Y F, Huang K F and Lan Y P 2002 *Phys. Rev.* E **66** 046215
[25] Chen Y F and Huang K F 2003 *Phys. Rev.* E **68** 066207
[26] Chen Y F, Lu T H, Su K W and Huang K F 2005 *Phys. Rev.* E **72** 056210